Electrical impedance of the hydrophobic oil-water interface: contactless measurement

Magdi H Saad[1,*], and Ali Habib Bashal[2]

[1] Department of Physics, Faculty of Science, Taibah University-Yanbu branch, KSA
[2]Department of Chemistry, Faculty of Science, Taibah University-Yanbu branch, KSA

DOI: https://doi.org/10.56293/IJASR.2022.5512

IJASR 2023
VOLUME 6
ISSUE 2 MARCH – APRIL **ISSN: 2581-7876**

Abstract: We have performed systematic contactless measurements aiming at the determination of the electrical impedance of an oil-water interface. The oil-water interface was formed within an insulin syringe tube due to the oil hydrophobicity. The measurement AC signal (0.1-300 kHz at 0.1 V) was capacitively coupled to the oil-water system through the syringe wall. The interface resistivity was estimated at ~$2\times10^{9}\Omega\cdot$m(assuming the interface as a slip layer with width ~ 10 nm) and was associated with hydroxide (OH^{-}) ions, agreeing with existing reports. The resistivity was found to be independent on the signal frequency, which may indicate the nonpolarized nature of the hydrophobic interface. The present impedance spectroscopy is important for hydrophobic systems and may give an insight into the future nondestructive (contactless) investigation of the electrical properties of the lipid layer in the living cell membrane.

Keywords: hydrophobicity, Oil-water interface, Impedance spectroscopy, contactless measurement.

1. Introduction

Hydrophobic materials (such as oil) are non-polar and, thus, have a weak affinity to water. Applications of hydrophobic materials are diverse [1] and include the renowned superhydrophobic self-cleaning surfaces [2] and anti-icing surfaces [3]. The hydrophobicity effect hasa direct impact on many chemicals (e.g.[4]), biological (e.g.[5]), and environmental (e.g.[6]) processes.Recently, the incorporation of materials that are hydrophobic (such as the reduced graphene oxide) and hydrophilic (a material witha strong affinity to water such as 2D graphene oxide) in a gas sensor has enhanced itssensing capability to overcome a challenging issue of distinguishing between tetrahydrofuran and dichloromethane[7].

These applications have stimulated fundamental research aiming at the investigation of the electrical properties of the hydrophobic interface. For instance, Tian *et al* [8] managed to experimentally find that the hydrophobic interface is negatively charged due to the high adsorption of the hydroxide (OH^{-}) ions at the interface. This finding has been supported by molecular dynamics simulations [9].Hydrophobic materials have also been utilized for controlling the metallic corrosion rate (e.g. [10] and [11]). The results of impedance spectroscopy measurements on Cu with hydrophobic coating have showna significant reduction in the corrosion rate in seawater [12].

To contribute to the ongoing fundamental research on the electrical characterization of the hydrophobic interface, this paper reports on the systematic contactless measurements of the impedance of the oil-water hydrophobic interface. We have used commercial olive oil and distilled water within insulin syringe. The oil-water interface was formed due to the oil hydrophobicity. The measurement AC signal was capacitively coupled to the oil-water system through the syringe plastic wall. We have previously used a similar contactless measurement technique to accurately determine the dependence of the conductivity on the size of gold nanoparticles [13]. In the present work, we used theSolarton Analytical 1287A and 1255B (see Fig. 1) Frequency Response Analyzer [14] which has good measurement accuracy and precision. The reactance of the plastic syringe wall $<100k\Omega$ at the measurement frequencies of 100 kHz $<f<$300 kHz, which allows sufficient portion of the measurement signal to penetrate the plastic wall into the oil-water interface. Hence, we have managed to estimate the resistivity of the interface at ~ $2\times10^{9}\Omega\cdot$m and found it to be consistent with ionic resistivity associated with OH^{-}in water, a result that conformswith existing investigations (e.g.[9]) that attribute the negative charge of the interface to the OH^{-} ions.

Besides being nondestructive and contamination-free, contactless impedance measurement has become an important method for the detection of inorganic or small organic ions in capillary electrophoresis [15]. Thus, we anticipate that our present work would open an interesting research avenue towards thenondestructive (contactless) investigation of hydrophobicity associated with a lipid layer (e.g. [16] and [17]) in the living cell membrane.

2. Measurement procedure and impedance model

Figure 1 shows a schematic of the measurement set-up consisting of the measuring instrument (Solarton Analytical 1287A and 1255B Frequency Response Analyzer [14]) from which the AC signal (100 mV, 0.1 – 300 kHz) is applied to the pair of Aluminum electrodes (Al electrodes) that are tightly wrapped around the syringe tube (inner diameter ~ 2 mm).Thus, the electrodes are capacitively coupled to the sample (oil-water) within the tube through the syringe plastic wall. We use commercial olive oil and distilled water. The effective length of the channel within the tube containing the sample is defined by the electrode-electrode separation whichwas$l$ ~ 1.5 cm. The hydrophobic interface prevents oil-water mixing.

The top part of Fig. 1 is the impedance model for the sample and the surrounding (external) electrical environment. The impedances Z_w, Z_o, Z_i, Z_p, and Z_x are for the water, oil, oil-water hydrophobic interface, tube wall, and external circuit (including parasitic ones).From the model, the effective measured impedancesfor a channel with water only, oil only, and oil-water samplesare respectively given by equations (1) – (3) below:

$$Z_{mw}^{-1} = Z_x^{-1} + \left(Z_p + Z_w\right)^{-1} \quad \text{..... (1)}$$

$$Z_{mo}^{-1} = Z_x^{-1} + \left(Z_p + Z_o\right)^{-1} \quad \text{..... (2)}$$

$$Z_{mow}^{-1} = Z_x^{-1} + \left(Z_p + \frac{Z_o}{2} + Z_i + \frac{Z_w}{2}\right)^{-1} \quad \text{..... (3)}$$

In equation (3), Z_o and Z_w are divided by 2 because the two halves of the channel were filled with oil and water. From eqns. (1) – (3) we deduce:

$$Z_i \approx \left(Z_{mow}^{-1} - Z_{ma}^{-1}\right)^{-1} - \frac{\left(Z_{mw}^{-1} - Z_{ma}^{-1}\right)^{-1}}{2} - \frac{\left(Z_{mo}^{-1} - Z_{ma}^{-1}\right)^{-1}}{2} \quad \text{..... (4)}$$

Where $Z_{ma} \approx Z_x$ is the measured impedance with empty tube (i.e. air-filled tube). This approximation holds because the empty tube has a significantly large capacitive reactance, hence, the measurement effectively gave rise to Z_x.

It is worth mentioning that the measured impedances in equation (4)were provided in terms of their measured real and imaginary parts. Therefore, a simple MATLAB© or Microsoft© Excel code was used to determine Z_i from the complex-number analysis of equation (4).

3. Results and discussions

Figure 2 (a) and 2(b) show the measured impedancesZ_{ma}, Z_{mw}, and Z_{mow} versus the frequency, f. To avoid crowding the space, we have not shown Z_{mo} because we observed thatZ_{mo} ~ Z_{ma}, indicatinghigh oil impedance due tolack of polarity. Clearly, the data is complicated due to the incorporation of the unwanted (parasitic) external impedance, Zx. However, as shown in section 2, we use the impedance model analysis to eliminate Z_x andextract the impedance of interest from the measurement data. For example, Z_i (oil-water interface impedance) was extractedin equation (4) and its real and imaginary parts ($\mathrm{Re}.Z_i$ and $-\mathrm{Im}Z_i$)areillustrated in Fig. 2(c)as a function of the frequency.Clearly, the real part (open blue triangles) is independent on the frequency (f) as can be seen from the red line which is shown as a guide for the eye. This suggests that the oil-water hydrophobic interface is dominantly resistive specifically because the imaginary part (open dark squares) did not follow the $1/f$ capacitive behaviour as, for instance, seen for the imaginary parts in Fig. 2(a) and 2(b). The ImZ_i may thus be associated with the residual of the calculation leading to equation (4). Such residual impedance may arise from the approximation Z_{ma} ~ Z_x and some hidden stray impedances.We observed similar residual imaginary part in a measurementof known resistances conducted to verify the accuracy of our model and the reliability of the measurement setup. This measurement will be discussed in conjunction with Fig. 3. We will show that the known resistances were measured with good accuracy regardless of the presence of this residual impedance.

Nevertheless, even if the observed Im.Z_i was physical, then $Z_i$may roughly resemblean idealsupercapacitor[18]that may be modelled[19] as a resistance, R, in series with a constant-phase-element, CPE[20] i.e. an imperfect capacitor.In this case, the impedance is characterized by a frequency-independent real part representing R, in an agreement with our data (Fig. 2(c)).However, we have not investigated the possibility of this series R-CPE model because the expected $1/f$behaviour ofIm. $Z_i$was obscured by the noisy$f$< 100 kHz region as seen in Fig. 2(c).

We stress thatwe have not observed signature of carrier diffusion across the oil-water interface that can be modelled using, for instance, Warburg diffusion elements [21].

In addition to the above-mentioned technical justifications, our assumption that the interface is dominantly resistive may be justified and supported by the molecular dynamic results by Kudin*et al*[9]which confirmed that the hydrophobic interface (between water and graphene)has a net negative charged, i.e. effectively nonpolar, as implied by the experiment (e.g.[8]). The absence of charge polarity at the interface may crudely regarded as a signature of a resistive interface that would otherwise exhibit a pronounced capacitive and, hence, frequency dependent contribution toZ_i.To arrive at a more decisive conclusion about the resistive nature of the oil-water interface, we need to construct and analyze a sophisticated model of a system of a charged interface between polar electrolyte (representing the water) and insulator (representing the oil). A similar model was the subject of recent research [22]on double-layer (DL) capacitance [23]which showed that the capacitance was independent of the system size. We assume that the change in system size corresponds to change in charge density, Q, at the interface with applied potential, ξ, from the AC signal. Thus, the interface capacitance ~ $dQ/d\xi$ ~ constant, resembling the equilibrium differential capacitance regime for the DL illustrated in Fig. 1 of Ref. #[24] with constant overall resistance. Our data in Fig. 2(c) is characterized by the constant Re. Z_i similar to the constant overall resistance in Ref.#[24]. Thus, be associated Re. $Z_i$with the interface resistance as follows.

We assigned the resistance of the hydrophobic interface to the real par tof Z_i, Re. Z_i.From Fig. 2(c), Re.Z_i~ 6MΩ. The resistivity of the interface was estimated as ρ_i ~(Re.Z_i)×A/ t ~ 2×10^{9}Ω·m, where A ~ 0.03 cm^2 is the cross-sectional area of the interface, t is the effective thickness of the interface assumed to be similar to the slip length ~ 10 nm as implied by Zhenbin*et al*[25] and Maali*et al*[26].Kudin*et al*[9] attributed the negative interface charge to the affinity of the negative hydroxide ions (OH^-) to the hydrophobic interface at low pH. We used commercial distilled water that has pH ~5 to 7. We assume that the interface has roughly the same OH^-concentration as that for the water (~ $10^{-14}/10^{-pH}$) whichranges from 10^{-9} to 10^{-7} molar. Consequently, the corresponding OH^- conductivities are between~$10^{-8}\Omega^{-1}$ m^{-1} and $10^{-6}\Omega^{-1}$ m^{-1}which were roughly estimated using the OH^- molar conductivity of 19.8×10$^{-3}\Omega^{-1}$m^2 mol^{-1}[27].According to our measurement, the hydrophobic interface conductivity =$1/\rho_i$ ~ $10^{-9}\Omega^{-1}$ m^{-1}which is consistent with the estimated range of conductivities for OH^- in water.

To check the reliability of our measurement and impedance models, we analyzed the model for Z_{mw}measurement. The objective is to estimate the capacitance of the syringe plastic wall, C_p, then compare it with the theoretical value ~ 4 pF for the cylindrical plastic wall (0.2 mm thick with dielectric constant ~ 3) of the syringe beneath the two electrodes (each ~ 2 mm wide). From equation (3) and Z_{ma} ~ $Z_x$we get$(Z_{mw}^{-1} - Z_{ma}^{-1})^{-1} = Z_p + Z_w = Z_{pw}$whichrepresents a series combination of Z_p(considered to be purely capacitive with capacitance C_p) and Z_w (considered as a parallel resistor (R_w)-capacitor (C_w) configuration (inset Fig. 2(d)).The main Fig. 2(d) shows that the real part, Re.Z_{pw}, vs. the imaginary part, Im. Z_{pw}, are nicely fit (blue and red lines, with impedance Z_{fit}) to the circuit model ofZ_{pw}shown in the inset of Fig. 2(d). From the fitting, Cp ~ 5 pF, R_w ~ 0.2 MΩ, and C_w ~ 10 pF.Clearly, C_p from the model fitting agrees very well with the theoretical value ~ 4 pF. The impedance analysis software used in Fig. 2(d) was the Matlab©Z-fit code [28].

To furthermore check the reliability of our model analysis (section 2) and measurement procedure, we used our measurement set-up to measure known resistances (R_k = 0.47, 47, or 94 kΩ, inset of Fig. 3) of resistors impeded between two impedances (Z_{left} and Z_{right}, inset of Fig. 3). This measurement aimed to emulate the extraction method of Z_i (hydrophobic interface impedance) discussed in section 2. Here, R_k, Z_{left}, and Z_{right} (inset of Fig. 3) played the roles ofZ_i, Z_o and Z_w (inset of Fig. 1), respectively. The results were then analyzed following similar proceduresas that presented in section 2, leading to the following equation (5) that resembles equation (4):

$$R_k \approx \left(Z_{mlr}^{-1} - Z_{ma}^{-1}\right)^{-1} - \left(Z_{ml}^{-1} - Z_{ma}^{-1}\right)^{-1} - (Z_{mr}^{-1} - Z_{ma}^{-1})^{-1} \quad \text{..... (5)}$$

Where Z ma ~ Z_x, and the measured impedances Z_{mlr}, Z_{ml}, and Z_{mr}, respectively, correspond to measurements on Z_{left}-R_k-Z_{right}, Z_{left} only, and Z_{right} only. The main Fig. 3 shows the extracted R_k values (red, blue and dark squares) using equation (5) versus the frequency. Interestingly, the extracted R_k values were frequency independent and matched the known R_k values with good accuracy.

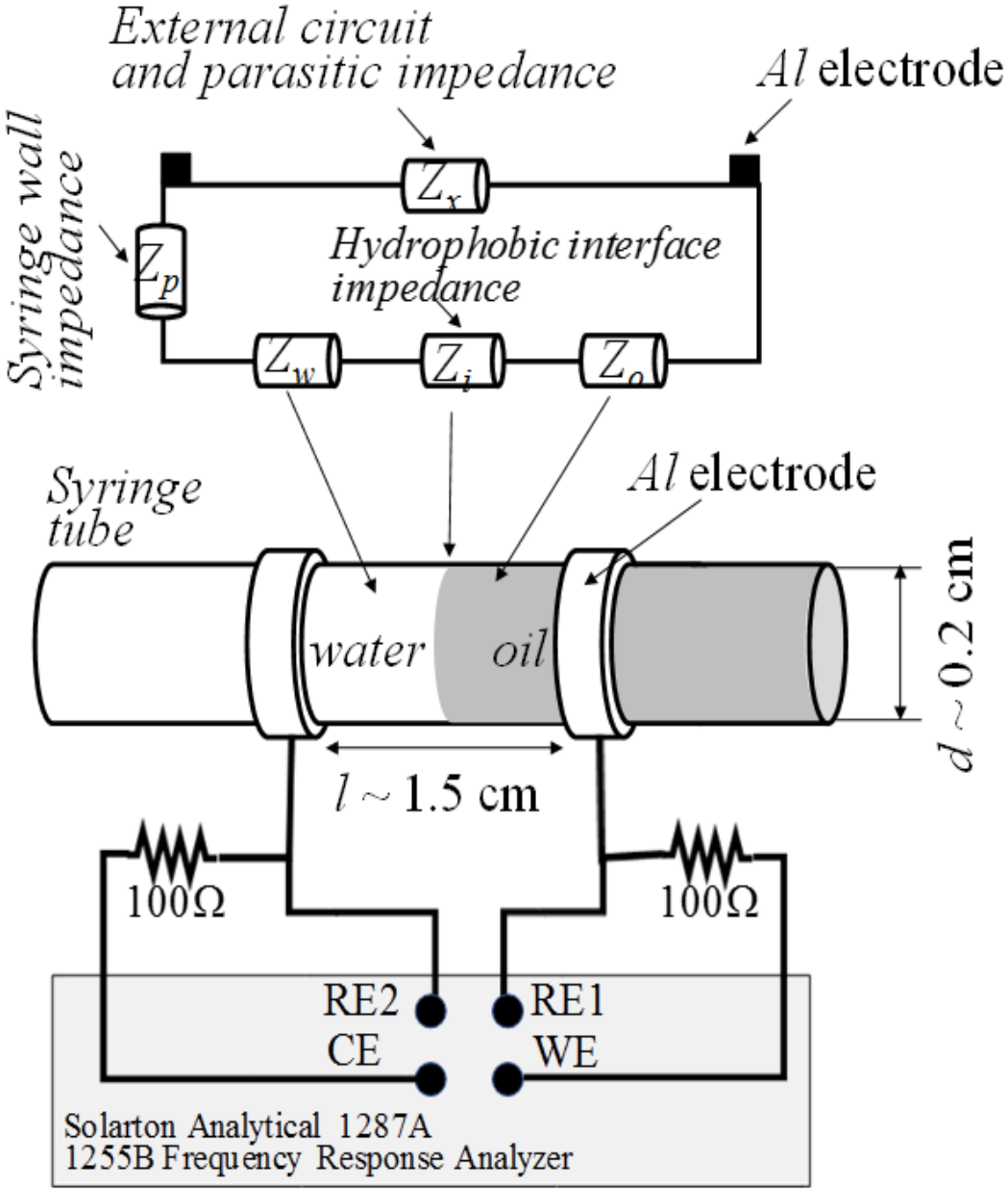

Figure 1: Schematic of the measurement set-up involving the impedance analyzer instrument (Solarton 1287A and 1255B). The sample (e.g. oil-water) is coupledcapacitively to the Al electrodes through the syringe plastic wall. CE, WE, RE1 and RE2 are respectively the counter, working, reference 1, reference 2 electrodes of the instrument. The top circuit diagram depicts the impedance model of the measurement set-up where the impedances Z_w, Z_o, Z_i, Z_p, and Z_x are for the water, oil, oil-water hydrophobic interface, tube wall, and external circuit (including parasitic ones).

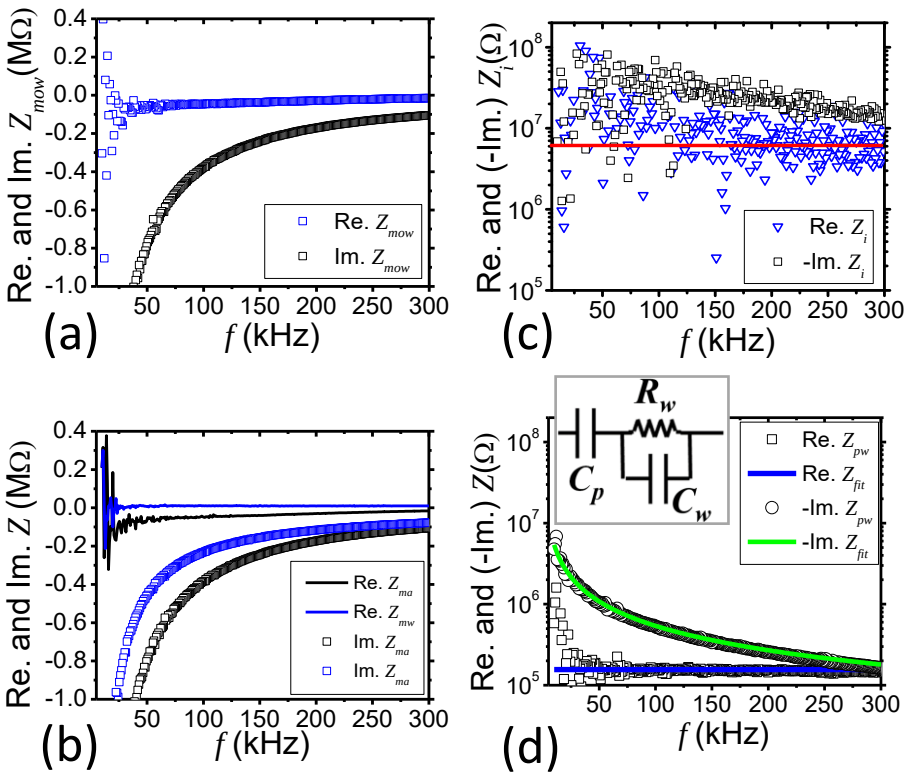

Figure 2: the measured impedances (Re. and Im. refer to real and imaginary impedance parts) versus the frequency, f, for (a) oil-water sample, Z_{mow}, and (b) empty tube, Z_{ma}, and water filled tube, Z_{mw}. (c) The hydrophobic interface impedance, Z_i, extracted using equation (4) (see text) (d) – Im. Z_{pw} and Re. Z_{pw} vs. f where Z_{pw} is the equivalent impedance of water impedance (Z_w≡ parallel R_w-C_w) in series with plastic tube impedance (Z_p≡ reactance with capacitance C_p). The green and blue lines are the fits (impedance ≡Z_{fit}) of the data using the circuit model shown in the inset with C_p = 5×10^{-12} F, C_w = 1×10^{-11} F, and R_w = 0.2 MΩ.

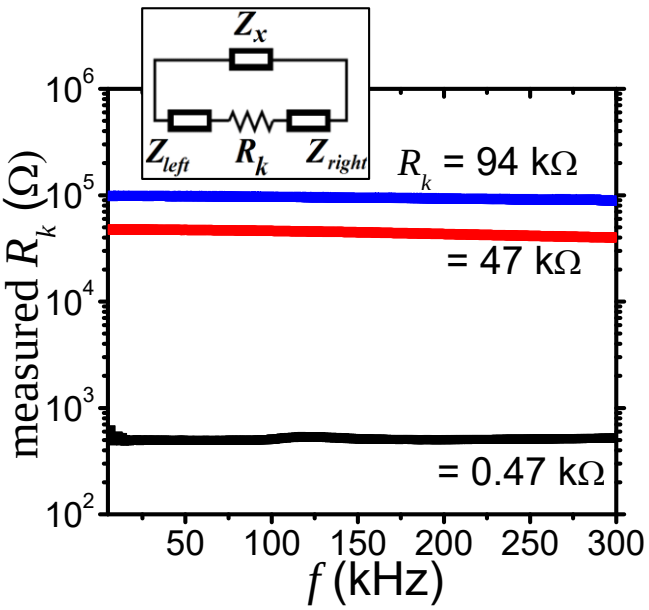

Figure 3: Measurement method of known resistances R_k = 0.47, 47, or 94 kΩ using the measurement setup of Fig. 1 where R_k were sandwiched in series between the impedances Z_{left} and Z_{right} (inset). The values of R_k (blue, red, black squares) extracted following similar model analysis as that presented in section 2 (see text).

4. **Conclusion**

Systematic contactless impedance measurements on oil-water interfacehave been performed at room temperature. The oil-water interface was formed within an insulin syringe tube due to the oil hydrophobicity. The measurement AC signal (0.1-300 kHz at 0.1 V) was capacitively coupled to the oil-water system through the syringe wall. The interface resistivity was estimated at ~ 2×10^9Ω·m (assuming the interface as a slip layer with width ~ 10 nm) from the measured equivalent impedances of the oil, water and empty tube and was found to be independent on the signal frequency, probably reflecting thenonpolarizednature of the hydrophobic interface. The present impedance spectroscopy is important for hydrophobic systems and may give an insight on future nondestructive (contactless) investigation of the electrical properties of the lipid layer in the living cell membrane.

References

1. D. Ahmad, I. van den Boogaert, J. Miller, R. Presswell, and H. Jouhara, "Hydrophilic and hydrophobic materials and their applications," *Energy Sources Part Recovery Util. Environ. Eff.*, vol. 40, no. 22, pp. 2686–2725, 2018.
2. M. Ma and R. M. Hill, "Superhydrophobic surfaces," *Curr. Opin. Colloid Interface Sci.*, vol. 11, no. 4, pp. 193–202, 2006.
3. L. Cao, A. K. Jones, V. K. Sikka, J. Wu, and D. Gao, "Anti-icing superhydrophobic coatings," *Langmuir*, vol. 25, no. 21, pp. 12444–12448, 2009.
4. R. Breslow, "Hydrophobic effects on simple organic reactions in water," *Acc. Chem. Res.*, vol. 24, no. 6, pp. 159–164, 1991.
5. C. Tanford, *The hydrophobic effect: formation of micelles and biological membranes 2d ed.* J. Wiley., 1980.
6. P. M. Gschwend and S. Wu, "On the constancy of sediment-water partition coefficients of hydrophobic organic pollutants," *Environ. Sci. Technol.*, vol. 19, no. 1, pp. 90–96, 1985.
7. S. Some *et al.*, "Highly sensitive and selective gas sensor using hydrophilic and hydrophobic graphenes," *Sci. Rep.*, vol. 3, p. 1868, 2013.
8. C. Tian and Y. Shen, "Structure and charging of hydrophobic material/water interfaces studied by phase-sensitive sum-frequency vibrational spectroscopy," *Proc. Natl. Acad. Sci.*, vol. 106, no. 36, pp. 15148–15153, 2009.
9. K. N. Kudin and R. Car, "Why are water- hydrophobic interfaces charged?," *J. Am. Chem. Soc.*, vol. 130, no. 12, pp. 3915–3919, 2008.
10. E. Vazirinasab, R. Jafari, and G. Momen, "Application of superhydrophobic coatings as a corrosion barrier: A review," *Surf. Coat. Technol.*, vol. 341, pp. 40–56, 2018.
11. M. Montemor, "Functional and smart coatings for corrosion protection: a review of recent advances," *Surf. Coat. Technol.*, vol. 258, pp. 17–37, 2014.
12. T. Liu, Y. Yin, S. Chen, X. Chang, and S. Cheng, "Super-hydrophobic surfaces improve corrosion resistance of copper in seawater," *ElectrochimicaActa*, vol. 52, no. 11, pp. 3709–3713, 2007.
13. M. Khalafalla*et al.*, "Size-dependent conductivity dispersion of gold nanoparticle colloids in a microchip: contactless measurements," *J. Nanoparticle Res.*, vol. 16, no. 8, p. 2546, 2014.
14. J. Harper, M. Rust, B. Sayers, A. Savage, and S. Analytical, "High-frequency, high-current impedance spectroscopy: experimental protocols enabling measurement up to 1MHz at high current densities," *Solartron Anal. Tech. Bull. Farnb. UK TBANALYTICAL001*, 2004.
15. P. Kubáň and P. C. Hauser, "Contactless conductivity detection for analytical techniques: Developments from 2016 to 2018," *Electrophoresis*, vol. 40, no. 1, pp. 124–139, 2019.
16. M. F. Osborn *et al.*, "Hydrophobicity drives the systemic distribution of lipid-conjugated siRNAs via lipid transport pathways," *Nucleic Acids Res.*, vol. 47, no. 3, pp. 1070–1081, 2018.
17. A. Biscans*et al.*, "Hydrophobicity of Lipid-Conjugated siRNAs Predicts Productive Loading to Small Extracellular Vesicles," *Mol. Ther.*, vol. 26, no. 6, pp. 1520–1528, 2018.
18. G. Wang, L. Zhang, and J. Zhang, "A review of electrode materials for electrochemical supercapacitors," *Chem. Soc. Rev.*, vol. 41, no. 2, pp. 797–828, 2012.
19. V. Uchaikin, R. Sibatov, and A. Ambrozevich, "On impedance spectroscopy of supercapacitors," *Russ. Phys. J.*, vol. 59, no. 6, pp. 845–855, 2016.

20. G. Brug, A. Van Den Eeden, M. Sluyters-Rehbach, and J. Sluyters, "The analysis of electrode impedances complicated by the presence of a constant phase element," *J. Electroanal. Chem. Interfacial Electrochem.* vol. 176, no. 1–2, pp. 275–295, 1984.
21. M. E. Orazem and B. Tribollet, "Electrochemical impedance spectroscopy," *AngewChemInt Ed*, vol. 48, pp. 1532–1534, 2009.
22. C. Zhang, "Communication: Computing the Helmholtz capacitance of charged insulator-electrolyte interfaces from the supercell polarization," *J. Chem. Phys.*, vol. 149, no. 3, p. 031103, 2018.
23. D. C. Grahame, "The electrical double layer and the theory of electrocapillarity." *Chem. Rev.*, vol. 41, no. 3, pp. 441–501, 1947.
24. B.-A. Mei, O. Munteshari, J. Lau, B. Dunn, and L. Pilon, "Physical interpretations of Nyquist plots for EDLC electrodes and devices," *J. Phys. Chem. C*, vol. 122, no. 1, pp. 194–206, 2017.
25. Z. Ge, D. G. Cahill, and P. V. Braun, "Thermal conductance of hydrophilic and hydrophobic interfaces," *Phys. Rev. Lett.*, vol. 96, no. 18, p. 186101, 2006.
26. A. Maali and B. Bhushan, "Measurement of slip length on superhydrophobic surfaces," *Philos. Trans. R. Soc. Math. Phys. Eng. Sci.*, vol. 370, no. 1967, pp. 2304–2320, 2012.
27. F. Johnston, "A textbook of physical chemistry (Adamson, Arthur, W.)," *J. Chem. Educ.*, vol. 51, no. 6, p. A345, 1974.
28. J.-L. Dellis, "MatlabZfit." [Online]. Available: https://www.mathworks.com/matlabcentral/fileexchange/19460-zfit. [Accessed: 06-Dec-2019].